ELSEVIER

Wear 236 (1999) 165–178

WEAR

www.elsevier.com/locate/wear

Chemical characterization of antiwear films generated by Tris-[*p*-(perfluoroalkylether)phenyl] phosphine using X-ray absorption spectroscopy

J.N. Cutler [a,*], J.H. Sanders [a], P.J. John [b], G. DeStasio [c], B. Gilbert [d], K. Tan [e]

[a] *AFRL / MLBT, Materials and Manufacturing Directorate, Wright Patterson AFB, OH 45433, USA*
[b] *University of Dayton Research Institute, Dayton OH, 45469 USA*
[c] *Istituto di Struttura della Materia, Consiglio Nazionale della Ricerche, Via Fosso del Cavaliere, I-00133, Rome, Italy*
[d] *Institut de Physique Appliquée, Ecole Polytechnique Fédérale, CH-1015, Laussane, Switzerland*
[e] *Canadian Synchrotron Radiation Facility, University of Wisconsin, Madison WI, 53589 USA*

Received 11 March 1999; received in revised form 25 June 1999; accepted 25 June 1999

Abstract

Perfluoropolyalkylethers (PFPAEs) are primary candidates as high temperature oils for the next generation of turbine engines due to their chemical and thermal stability. However, the usefulness of the PFPAE base fluids are hindered by corrosive wear in dry environments. This problem can be minimized and overall wear properties improved by the addition of soluble additives, such as Tris-[*p*-(perfluoroalkylether)phenyl] phosphine (PH3). Currently, little work has been reported on the mechanism by which this additive actually improves overall wear performance. This paper provides critical insight regarding the interactions of the PFPAE additive PH3 with Fe-based alloys in a pin-on-flat tribological environment. It is found that the PH3 decomposes on the surface, within the wear track, forming a tribofilm composed of a polyphosphate glassy material. At low relative humidity ($\sim$ 0%), the polyphosphate antiwear film substantial improves the wear performance of the fluid which is reflected by a decrease of $\sim$ 325% in width of the measured wear scar. Contrasting this result, at high relative humidity ($\sim$ 50%), little improvement is found in the wear properties of the fluid. This is due to the formation of carboxylate multilayers produced by PFPAEs in a moist environment, which serve as their own antiwear film. The formation and protective properties of these films are controlled by three important environmental factors. First, oxygen must be present in order to form the polyphosphate. Second, tribomechanical scission and hydrolysis of the additive is required to drive the reaction to completion. At low humidity, a large amount of unreacted and intermediate material was found within the wear track. Third, the test temperature combined with the relative humidity was shown to control the overall useful lifetime of the additive. In order to gain some understanding on how this additive works, a series of tribological experiments were performed at different temperatures, relative humidities and rubbing times. The worn specimens were examined by X-ray absorption near edge structure spectroscopy (XANES) and imaging photoelectron spectromicroscopy (MEPHISTO).

Keywords: Antiwear films; Tris-[*p*-(perfluoroalkylether)phenyl] phosphine; X-ray absorption spectroscopy

1. Introduction

To meet the ever-increasing demands of advanced aircraft design, new technologies must be developed. This basic axiom is true in the field of tribology as it applies to the development of high performance turbine engines. To achieve higher thrust-to-weight ratios in new jet aircraft engine designs, operation temperature must be increased beyond the level where current oils are useful. A primary candidate fluid for this task is the perfluoropolyalkylethers (PFPAEs) due to their low volatility, excellent high temperature oxidative stability, acceptable viscosity index and relative inertness to system materials [1–5]. For example, they are currently utilized as fluids in mechanical and thermal (diffusion) vacuum pumps and as topical lubricants in the rigid magnetic media in the computer disk industry [6]. Success in these applications suggest they have potential in turbine engines [7].

Although PFPAEs have shown a great deal of promise as a hydrocarbon replacement in turbine engines, they are known to have two major shortcomings. They decompose under sliding contact to form metal fluorides, both on the

* Corresponding author

0043-1648/99/$ - see front matter
PII: S0043-1648(99)00283-5

surface in the form of FeF_3 and subsurface below the iron oxide in the form of FeF_2. It is generally accepted that these metal fluorides provide Lewis acid sites that act as a catalyst to accelerate decomposition of the fluid and increase the rate of surface corrosion and wear [8–20]. In an attempt to quench this decomposition process, a PFPAE must be tailored for its particular application by the addition of soluble additives [21–23]. The second problem is common to synthetic oils: they do not have good boundary lubrication properties. This is complicated by the difficulty in finding additives soluble in fluorinated compounds.

Over the past several years, additives have been developed which improve corrosion resistance and appear to generate lubricious surface films in sliding environments. Until recently, the mechanism by which these additives worked to improve overall oxidation–corrosion performance was not clearly understood. Work by several groups [3,4,23–28] have cast some light on the mechanism of corrosion protection and the lubricious properties generated by these new additives. More recently, Cutler et al. [21] and John et al. [24] have hypothesized that these additives act as a diffusion barrier by either forming a chemisorbed layer or a decomposition film on the surface. This surface layer prevents the direct interaction of the PFPAE with the iron-containing substrate thereby terminating the corrosion process. However, little work has been reported on the mechanism by which these additives improve overall wear performance [23].

To aid in the development of future high temperature PFPAE additives, an understanding of the overall antiwear mechanism associated with the current class of additives is crucial. As a model, this work focuses on the tribological properties of the fluorinated additive Tris-[*p*-(perfluoroalkylether)phenyl] phosphine (PH3). Originally, PH3 was developed to inhibit corrosion but serendipitously was found to have good antiwear properties. Previously, Cutler et al. [21] showed that PH3 obtains its corrosion protective properties by the formation of a polyphosphate surface layer. Similar type polyphosphate layers have been observed in hydrocarbon-based antiwear films formed by zinc dialkyldithiophosphate [29–32] and tricresylphosphate [33]. To see if hydrocarbon additive models apply to PFPAE additives, a study of the antiwear properties and resulting surface films generated by PH3 have been examined by X-ray absorption near edge structure (XANES) spectroscopy and imaging photoelectron spectromicroscopy microscope à emission de photoélectrons par illumination synchrotronique de type onduleur (MEPHISTO). In recent years, Yin et al. [29,30], Fuller et al. [31] and Kasrai et al. [32] have shown that XANES spectroscopy is a powerful tool to aid in the characterization of lubricious films. By detecting electronic transitions between occupied core levels and unoccupied states below and above the vacuum level of the absorbing species, XANES has been used to examine subtle changes in the local chemical environment of the element that is being probed. The spectra are a fingerprint of the chemical nature of the film when compared to model compounds of known local chemical environments [34]. Combining total electron yield (TEY) and fluorescence yield (FY) techniques, they have been able to examine the outermost surface (~3 nm) and bulk (~50 nm) chemical composition of tribofilms in a non-destructive manner.

In this vein, we are using XANES spectroscopy and imaging photoelectron spectromicroscopy to examine the effect of temperature, humidity and rubbing time on the chemistry and related surface distribution of the PH3 additive and its associated decomposition products.

2. Experimental

The base fluid used for these experiments was a linear PFPAE, Demnum S-65, produced by Daikin Industries, which has a backbone structure of $CF_3CF_2CF_2(OCF_2CF_2CF_2)_mOCF_2CF_3$ and was used without further purification. The additive was a substituted PH3 (80%) and Tris-[*p*-(perfluoroalkylether)phenyl] phosphineoxide (20%) mixture (I),

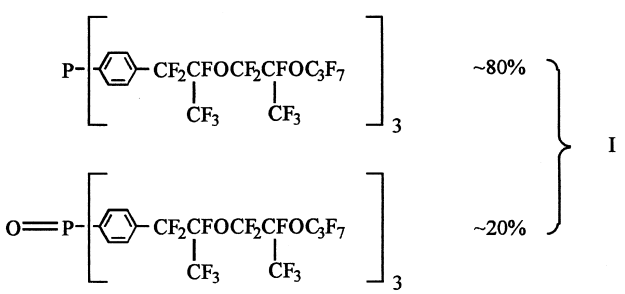

which was prepared in-house with a purity of > 90% [35]. The formulation used to produce the tribological samples was prepared by dissolving 1% of the additive by weight in the Demnum S-65 base stock.

The tribofilms examined in this study were generated on M-50 steel in a Plint reciprocating wear rig. The flat was a 12.7 mm diameter by 7.75 mm thick disk with a Rockwell hardness of ~60. The average surface roughness, R_a, was less than a 0.5 μm. The pins were 6 mm diameter by 6 mm length bearing rollers. The cylindrical pin was loaded against the coupon in the oil containing the additive and was rubbed for the desired length of time. The most commonly used test variables were temperature 150°C, speed 6 Hz, load 250 N, relative humidity of 0% or 50%, stroke 9 mm and rubbing times of 5 min to 6 h. The coefficient of friction, μ, and contact resistance were recorded continuously during the run and the coefficient of friction quoted is the average value over the final 10 min of the run. After the test, the coupon was ultrasonically cleaned in Freon-TF, 1,1,2-trichlorotrifluororethane, for 20 min. The film generated on the coupon was used for the

XANES analysis and the cylindrical pin was used for the wear scar measurements.

2.1. X-ray absorption spectroscopies

2.1.1. XANES spectroscopy

The Plint samples were examined by XANES spectroscopy. The XANES spectra were collected at the Canadian Synchrotron Radiation Facility (CSRF) [36] located on the 1 GeV storage ring, Aladdin, at the Synchrotron Radiation Center in Stoughton, WI. The P L-edge spectra were recorded using the grazing incidence Grasshopper soft X-ray beamline equipped with a 1800 groove/mm ruled grating which gave a practical photon resolution of < 0.2 eV. The P K-edge spectra were recorded using the double crystal monochromator beamline (DCM). The synchrotron radiation was monochromatized using InSb crystals with a photon resolution of ~ 0.9 eV.

The photoabsorption spectra were recorded in both total electron yield (TEY) and fluorescence yield (FY) modes. The experimental setup has been described in detail in an earlier paper [37]. In short, the total electron yield spectra were collected by directly measuring the sample current generated by the incident photons. Fluorescence yield spectra were recorded by measuring the emitted fluorescence photons and were detected by a chevron multichannel plate detector. In this paper, only total electron yield data will be reported, providing surface information primarily from the topmost 3 nm. The fluorescence yield data usually gives more bulk film information and its sensitivity probes the top 50 nm of the film. However, in this case, the signal was too weak.

The photon energy scale for the Grasshopper monochromator was referenced to the lowest P L-pre-edge peak of sodium metaphosphate, $Na_3P_3O_9$, at 136.5 eV. Likewise, the DCM beamline was calibrated using zinc phosphate, $Zn_3(PO_4)_3$, at 2151.6 eV. The relative energy scale was reproducible within ± 0.1 eV. All the spectra presented here represent the average of at least three scans.

2.1.2. MEPHISTO photoelectron spectromicroscopy

The photoelectron spectromicroscopy experiments were conducted on the 1 GeV storage ring Aladdin located at the Synchrotron Radiation Center in Stoughton, WI. The images were collected using the MEPHISTO imaging photoelectron spectromicroscope that has been discussed in detail previously [38]. In short, it is composed of the photon source (monochromatized soft X-rays from a synchrotron bending magnet source) and the electron optics, at 60° from the beamline and perpendicular to the sample surface. The electron optics accelerate and magnify the photoelectron beam emitted by the sample surface. A series of two microchannel plates and a phosphor screen intensify and convert the photoelectron magnified image into a visible image, which is then collected by a CCD camera and video acquisition system.

Several design improvements [38,39] concerning the electrostatic lens configuration, the large voltage in the electron optics, and the insertion of interchangeable apertures in the back focal plane of the objective lens have yielded a lateral resolution of 20 nm [39]. As to the spectroscopy performances, X-ray absorption spectra were taken with an photon energy resolving power up to 2000 (estimated limit depending on the beamline: 10^4) on both the 6 and 10 m torodial grating monochromator (TGM) beamlines. The MEPHISTO spectromicroscope has been successfully tested both in the photoemission and in the transmission modes [38,40]. The results presented here were obtained in the photoemission mode.

3. Results and discussion

3.1. Tribochemical films

3.1.1. XANES

Fig. 1 shows representative P L-edge XANES total electron yield (TEY) spectra of two antiwear films produced by the Plint reciprocating wear rig (150°C, 2 h, 250 N load) at low and high relative humidities, 0% (B) and

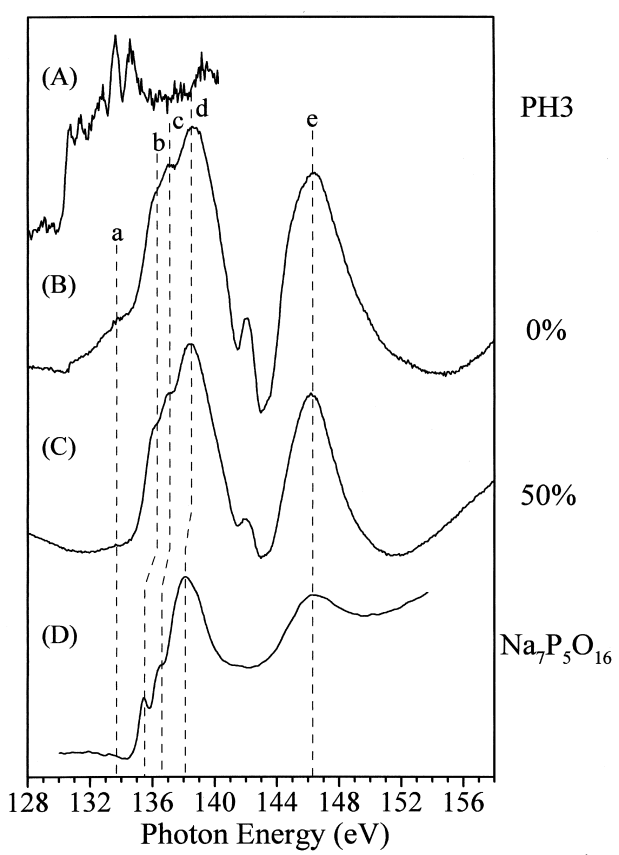

Fig. 1. P L-edge XANES (TEY) spectra of two tribofilms films produced at 150°C, 250 N load, 2 h of rubbing and two different relative humidities (0% and 50%) using 1% PH3 in Demnum, as compared with model compounds.

50% (C), along with the fresh additive (A) and a standard polyphosphate glass (D). The peak at ~142 eV in Fig. 1B and C is due to the C K-edge absorption at ~284 eV which is an artifact of the monochromator caused by second-order light from the grating.

Comparing Fig. 1A–D, it is immediately apparent that the additive has undergone a chemical transformation to a long chain length polyphosphate. The spectra of the two antiwear films are composed of four principal peaks labeled (b) through (e), at 136.3, 137.1, 138.5 and 146.3, respectively, which are characteristic of a polyphosphate. Peak (e) originates from the presence of a shape resonance generated by the bonding of the P atom to four electronegative oxygen atoms and is characteristic of a polyphosphate. In tetrahedral symmetry, peaks (b) through (d) are due to electronic transitions from the P L-edge to empty antibonding orbitals [29] of a_1 and t_2 symmetry. Peaks (b) and (c) are transitions into the spin–orbit split a_1 orbital and the broader peak (d) is a transition into an orbital of t_2 symmetry. Yin et al. have shown that the ratio of intensities for peaks (b) and (c) compared to peak (d) correlate with the overall number of phosphorus atoms found in the polyphosphate structure [29,30]. Based on their work, the antiwear film generated by the Plint reciprocating wear rig appears to be a long chain polyphosphate with an average chain length greater than twenty phosphorus units.

The top spectrum (A) in Fig. 1 is composed of several lines centered at approximately 133.5 eV and are representative of the PH3 additive. When the spectra of the 0% and 50% relative humidity samples are compared, a strong shoulder (a) is present on the low photon energy side of peak (b) in the low humidity sample (B). This band centered at roughly 133.7 eV is in good agreement with the overall centroid of the peaks that compose the starting material. Unlike the starting material, the shoulder is not composed of the several sharp resonances seen in the in the PH3 spectrum. This convoluted broad peak at 133.7 eV hints at the presence of numerous intermediate phosphate species existing during initial tribofilm formation.

At high humidity (C), there is little evidence of a shoulder on the low photon energy side of peak (b) implying that the reactions involved in the formation of a good polyphosphate tribofilm have gone further towards completion. In this regard, it has been observed that the stability of several different phosphorus-containing additives other than PH3 were strongly influenced by the amount of moisture they were exposed to during long term storage (unpublished data). The fact that water plays an important role in tribofilm formation and affects the long term storage of phosphorus additives in general suggests that hydrolysis of the PH3 additive is a key step in film growth.

The fluorescence yield (FY) data were collected but not reported since the signal was very weak. Due to the probing depth of the fluorescence yield technique (~50 nm), the lack of signal implies that the antiwear film formed within the wear track is very thin, on the order of 5 nm or less.

3.1.2. Effect of rubbing time and humidity

Fig. 2 shows a series of spectra obtained from antiwear films generated in the Plint recriprocating wear rig at different relative humidities, 0% (B–E) and 50% (F–I), and rubbing times of 5 min, 30 min, 2 h and 6 h in

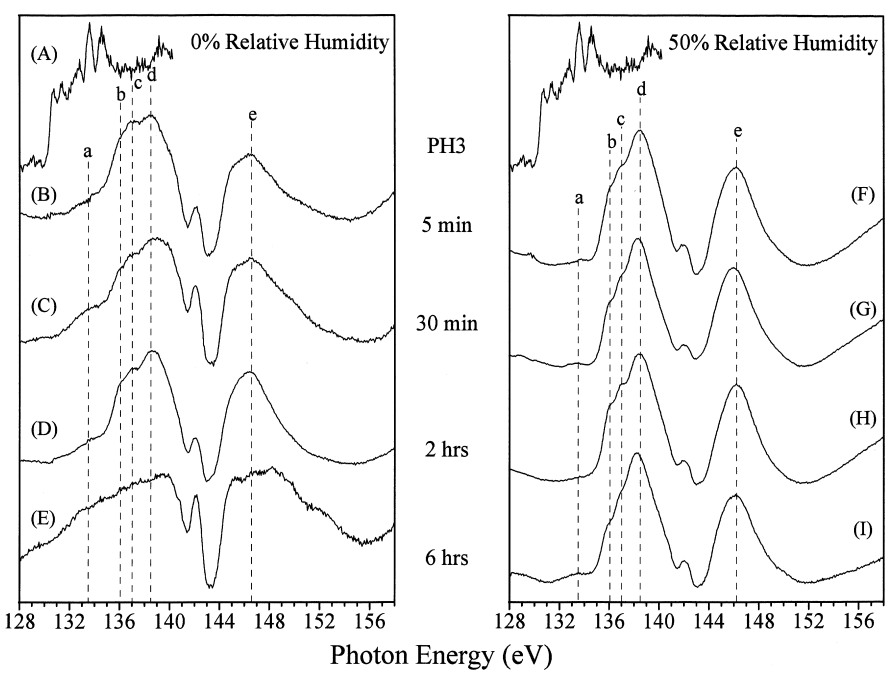

Fig. 2. P L-edge XANES spectra of tribofilms generated by 1% PH3 as a function of humidity and rubbing time, as compared to the starting material.

comparison to the starting additive (A). At high humidity, the spectra of the antiwear films indicate a polyphosphate material that is independent of rubbing time. As discussed above, the spectra of the tribofilms are composed of four characteristic peaks, (b)–(e). Even after only 5 min of rubbing (Fig. 2F), little evidence of unreacted or intermediate decomposition material is seen within the film, line (a). The average chain length of the polyphosphate appears to be independent of rubbing time and it is only after 6 h of rubbing that the average chain length of the polyphosphate slightly decreases.

In contrast, the spectra associated with the low humidity samples do show some marked differences in the surface tribofilm character as a function of rubbing time. First, the spectrum of the film produced after 5 min of rubbing (Fig. 2B) appears to be a very long chain length polyphosphate which decreases in average length as rubbing time is increased. This is reflected by the progressive decrease in intensity of peaks (b) and (c) from the 5 min tribofilm (Fig. 2B) as compared to the 2 h tribofilm (Fig. 2D). Second, the lifetime of the tribofilm is shorter at low humidity when compared to a higher humidity film. After 6 h of rubbing, there is no phosphorus signal evident in the L-edge spectrum of the low humidity sample (Fig. 2E). In comparison, the 6 h tribofilm at 50% relative humidity still shows a strong polyphosphate spectrum (Fig. 2I).

In order to understand the effect of moisture on the amount and lifetime of deposited phosphate in the wear scar, P K-edge data were recorded for the various Plint samples under different environmental conditions. Fig. 3 plots rubbing time vs. intensity of the P K-edge jump at 0% (Fig. 3A) and 50% (Fig. 3B) relative humidity. A typical P K-edge spectrum is shown in the insert of Fig. 3B. The spectrum is composed of a single peak, referred to as the white line, which is due to an electronic transition from the P 1s orbital to an orbital of e-type symmetry. The intensity of this edge jump is a function of the surface coverage of phosphorus. Two things are immediately apparent in Fig. 3 when the low and high humidity data are compared. First, the surface film formed at low humidity has an order of magnitude less signal due to phosphorus on the surface than at high humidity. The amount of phosphorus builds up for the first 2 h and then slowly decays away. After 6 h of rubbing, as shown in Figs. 2 and 3A, the amount of phosphorus has dropped substantially and the L-edge signal is undetectable. The disappearance of the antiwear film at low humidity indicates that the polyphosphate glass is easily removed from the surface. Second, the amount of phosphorus at high humidity reaches a constant value after the first 30 min and remains steady for the next several hours of testing.

Two different mechanisms may account for the surface concentrations. Karis et al. [41] and Liang and Spikes [42] observed the formation of mechanochemical scission products (e.g., $CF_3CO_2^-$) when PFPAEs where placed in a high shear environment. The presence of water at high humidity when combined with molecular shear leading to bond scission of a C–P bond within the additive accelerates the hydrolysis of the resulting fragments and direct growth of the surface polyphosphate. The resulting thicker phosphate

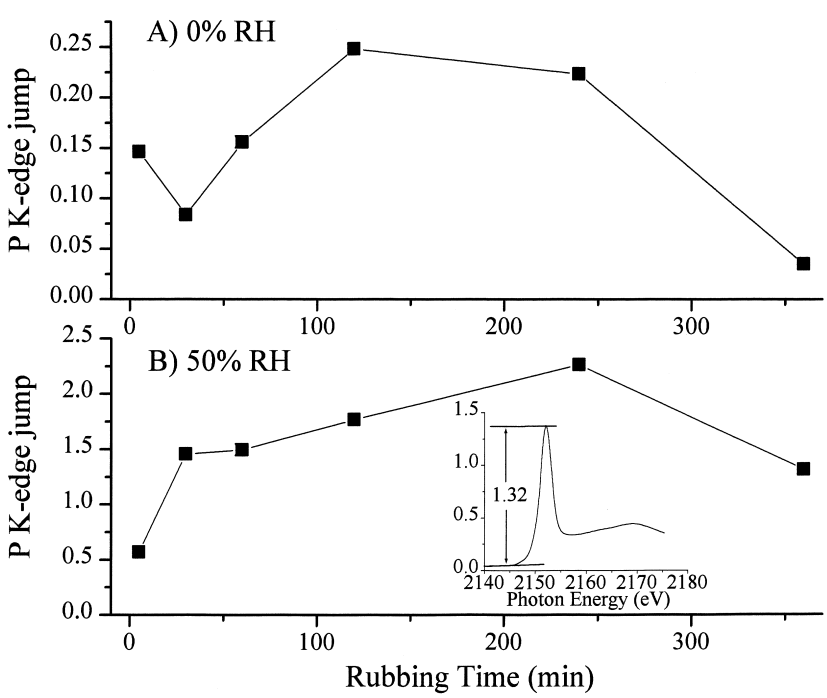

Fig. 3. The magnitude of the P K-edge jump of tribofilms generated by PH3 as a function of rubbing time at two different humidities. The insert in (B) shows a typical P K-edge spectra of a tribofilms generated by PH3.

film leads to better wear properties. At low humidity, the film contains a large amount of unreacted material and phosphate intermediates that may decrease the stability of the film. The alternate mechanism is connected to an accumulative effect between the fluid and additive. Liang et al. [43,44] showed that carboxylate multilayers are formed at high humidities and have excellent wear protective properties, thereby protecting and aiding in the growth of the surface phosphate film. The absence of the PFPAE multilayers at low humidity (Fig. 3A) allows for the dynamic removal of the phosphate film and the rapid degradation of the overall wear properties of the additive.

3.1.3. Wear and friction

To gain insight into the stability and functionality of the surface films formed by the PH3 additive, Fig. 4 plots the wear scar values and coefficients of friction against rubbing time for the PH3 formulated Demnum at low and high relative humidities (filled and open squares, respectively) along with data from 2 h of rubbing in unformulated Demnum (filled and open circles). At low humidity (Fig. 4A, filled squares), the wear scar width grows in a linear fashion with rubbing time. When compared to unformulated Demnum, the additive substantially improves the tribological usefulness of the fluid during 2 h of rubbing. The measured wear scar (220 μm) is visibly smaller than the 729 μm scar produced by the unformulated fluid. This shows a 325% improvement in wear.

The large wear scar produced by unformulated Demnum at low humidity was explained by Çavdar et al. [15] and Helmick et al. [23]. They showed that at low humidity unformulated PFPAEs sustained a large amount of corrosive wear due to the formation of acyl fluorides which accelerate the wear rate experienced by the pin. This corrosive wear was related to the formation of a subsurface FeF_2 layer which was formed by the interaction of acyl fluorides with trace moisture [19]. Consequently, the PH3 additive, at low humidity, appears to hinder corrosive wear by the formation of a polyphosphate layer. Similar results have been seen in an oxidation–corrosion study with PH3, where a polyphosphate layer was formed on M-50 steel and acted like a diffusion barrier preventing the PFPAE from reacting with the surface [21,24].

The coefficients of friction reported in Fig. 4B (filled squares) appear to be independent of rubbing time and ranged from 0.12 to 0.14. The PH3 additive slightly improved (~ 20%) the overall coefficient of friction when compared to the unformulated fluid which has an overall coefficient of friction of 0.16. This improvement could be associated with the lubricious character of the polyphosphate film formed in the wear track.

Fig. 4 shows the pin wear scar (Fig. 4A, open squares) widths and coefficients of friction (Fig. 4B, open squares) of the formulated fluid at 50% relative humidity. The wear scar initially increases in width as a function of rubbing time and seems to reach a steady state value of approxi-

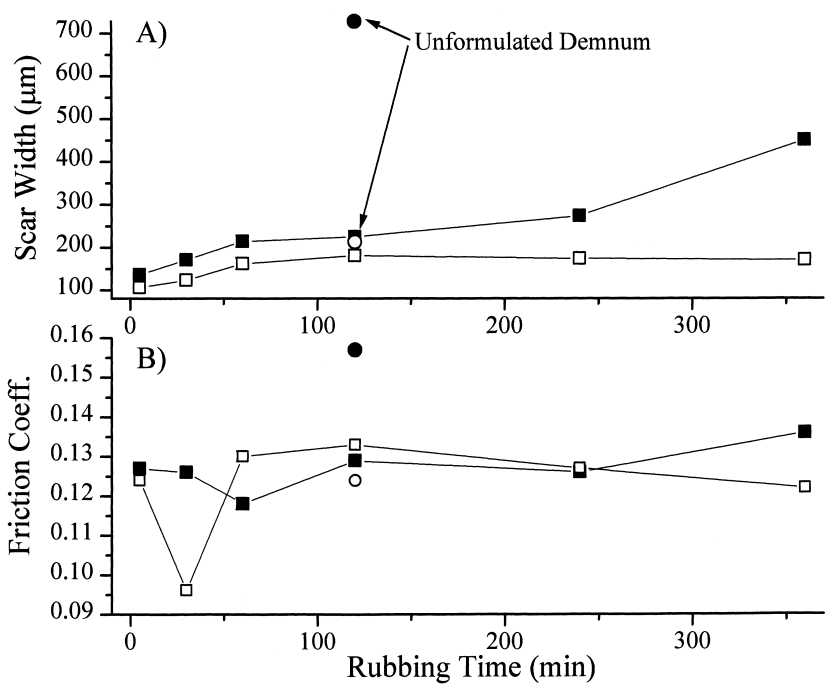

Fig. 4. Wear scar width and coefficient of friction measurements of tribofilms as a function of rubbing time generated by PH3 at two different humidities. (A) shows the wear scar widths and (B) shows the coefficient of frictions at 0% and 50% relative humidities, filled (■) and open squares (□), respectively. The (●) and (○) represent the wear scar width and coefficient of friction, respectively, of the unformulated fluid at 150°C, 250 N load and 2 h of rubbing at two different humidities.

mately 175 μm. When compared to unformulated data, the wear scar produced after 2 h of rubbing in a formulated fluid does not show the striking improvement (25%) in overall wear properties that were seen at low humidity (325%). The small improvement in wear scar width is further evidence of an accumulative effect between the polyphosphate tribofilm and the formation of carboxylate-based multilayers produced by Demnum [39,40] which have their own wear protecting properties.

3.1.4. Effect of temperature

Fig. 5 shows the antiwear films formed in the reciprocating wear rig when the rubbing time was held constant at 2 h and the temperature was varied from 125°C to 225°C. At low humidity, the stability of the film is strongly influenced by the temperature of the test. At intermediate temperatures, 150°C to 200°C, the antiwear film formed is composed of a polyphosphate containing a large portion of unreacted material. At 125°C and 225°C, the phosphate film does not appear to have formed on the surface which is reflected by the lack of structure at the P L-edge. Since a good polyphosphate film forms at intermediate temperatures, this would infer that the film is not very stable at the higher and lower temperature limits.

At high humidity and temperatures greater than 125°C, the antiwear film formed in the wear track is a polyphosphate and is chemically independent of temperature. At 125°C, the surface film contains a large quantity of unreacted and intermediate material (line (a)). Line (d) is much broader than in the higher temperature spectra and the shape resonance, line (e), is very weak. The increased broadness of line (d) may be related to a high second order carbon signal implying that a large amount of carbonacious material is present in the film.

Fig. 6 shows a correlation between surface phosphorus concentration and wear scar width as a function of experimental temperature for the low (A) and high (B) humidity data shown in Fig. 5. Similar to the data discussed in Fig. 3, the surface coverage of phosphorus is very low at 0% relative humidity. It is immediately apparent that the surface coverage appears to start low, at 125°C, reaching a maximum at 150°C and steadily decreasing as the temperature is increased. The open circles show the effect of temperature on the wear scar widths. When correlated with the unformulated data in Fig. 4, the width of the wear scar appears to be controlled by the presence of a polyphosphate surface layer. It is not until the experimental temperature reaches 200°C that the wear increases dramatically. The rapid increase in the wear rate may be due to a thermal/shear-related instability in the polyphosphate film. Two noteworthy observations can be drawn from this data. First, the additive helps in dry conditions by retaining good antiwear properties up to a temperature of 200°C. This is reflected by the small variation in wear scar as a function of temperature. Second, although the surface coverage has decreased at high temperatures, the thin antiwear film formed provides adequate antiwear protection.

Fig. 6B shows the influence that temperature plays on the antiwear properties of the PH3 additive in a high humidity environment. As seen in Fig. 3, the high humid-

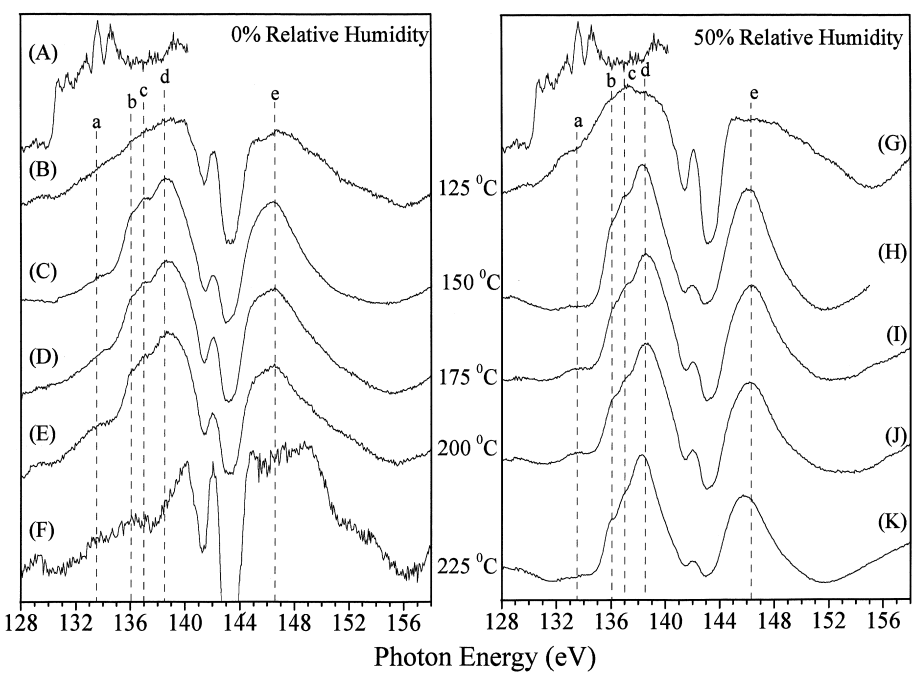

Fig. 5. P L-edge XANES spectra of tribofilms generated by 1% PH3 as a function of humidity and temperature, as compared to the starting material.

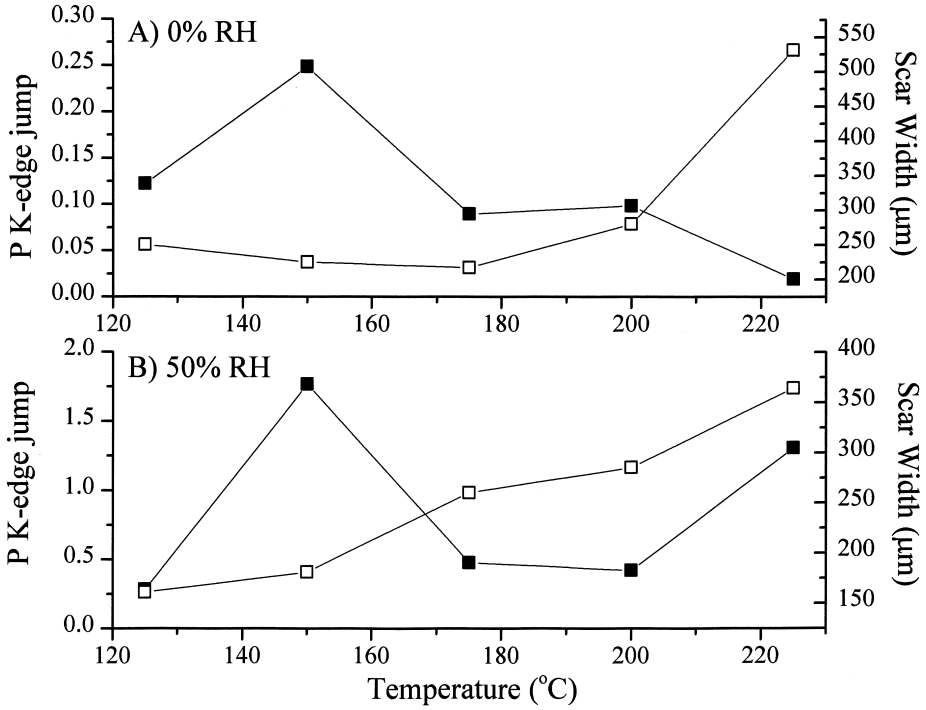

Fig. 6. P K-edge jump and wear scar width of tribofilms as a function of temperature generated by PH3 at two different humidities. The (■) represents the P K-edge jump and the (□) represents the coefficient of friction.

ity samples tend to have approximately a factor of ten times more phosphorus on the surface with a maximum coverage occurring at roughly 150°C. In contrast to the low humidity data, the wear scar widths appear to have some dependency on the experimental temperature, by increasing in width. Similarly, unformulated Demnum shows a temperature dependency with wear rate reflected by the decreasing stability at higher temperature of the carboxylate multilayers formed in the presence of moisture. At 200°C, the wear scar widths at low and high humidity are both approximately 300 μm. The increased width is due to the relative difference in phosphorus concentration between the two humidities. The coverage has decreased from a factor of ten at 150°C to a factor of approximately five at 225°C. This may be due to the decreasing effectiveness of the carboxylate multilayers to act as an antiwear species thereby leading to excessive wear of the phosphate film.

3.1.5. Effect of oxygen

Fig. 7 shows a series of antiwear and thermal films produced by the PH3 under different environmental conditions and temperatures. The top spectrum (A) is of the starting material and serves as a reference for the type and quantity of additive decomposition. In order to examine the importance of oxygen in the formation of an antiwear film, a Plint sample was prepared in an oxygen deficient environment (D). In similar work with ZDDP in a hydrocarbon fluid, the presence of nitrogen strongly influenced the effectiveness of the additive and the nature of phosphorus found on the surface. It was inferred from this result that oxygen was a key component in the formation of a

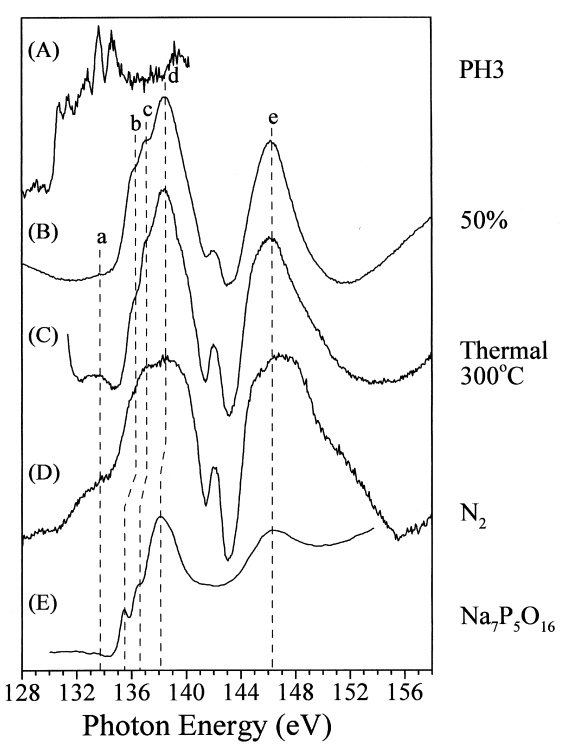

Fig. 7. P L-edge XANES spectra of thermal (300°C) and tribofilms (50% relative humidity and N_2 environment) generated by 1% PH3, as compared with model compounds.

Table 1
Experimental results from Plint tribometer and P L-edge jump intensity for low (0%) and high (50%) humidity samples in air and nitrogen environments

	0%	50%	N_2
Scar width (μm)	225	181	349
Friction coefficient	0.129	0.133	0.135
Contact resistance (Ω)	24K	37K	84
Edge jump	0.33	0.76	0.20

good polyphosphate film from ZDDP [45]. In initial experiments, an environmental enclosure surrounding the tribometer head was back-filled with nitrogen gas. The resulting wear data and corresponding L-edge spectra (not shown) were consistent with polyphosphate films formed at low humidity in air. The formation of a polyphosphate film can be explained by the high solubility of oxygen in a fluorinated fluid [46].

In order to understand the influence of oxygen on film formation, the fluid was deaerated by bubbling nitrogen gas through the fluid for approximately 45 min prior to rubbing. Fig. 7D shows the XANES spectrum obtained from the film formed on the surface and Table 1 shows a comparison between low and high humidity samples done in air and in a nitrogen environment. Table 1 shows that the wear scar width has increased ~75% (more wear) and the contact resistance has dropped to value that is consistent with metal-to-metal contact. In order to understand the surface film formed within the wear scar, the oxygen deficient film (Fig. 7D) is compared to the film formed in air (Fig. 7B). First, peaks (d) and (e) in Fig. 7D are much broader than in Fig. 7B due to the presence of carbon (second-order C K-edge data) within the surface film. The high photon energy shoulder on peak (e) is due to a fluorinated carbon from the additive and PFPAE fluid which is consistent with a poorly formed film. Second, peak (a) is very strong and is associated with phosphorus found in the starting material. Thirdly, peaks (b) and (c) are much stronger in intensity, indicating the presence of a very long chain length polyphosphate. Qualitatively, the film formed in a nitrogen environment is chemically similar to the film formed at lower temperatures, 125°C, in 50% relative humidity (see Fig. 5G).

3.1.6. Thermal films

In order to further the understanding of additive decomposition and factors that influence its stability and mechanism of formation, a series of thermal films were prepared by submerging an M-50 steel coupon into a linear PFPAE fluid formulated with PH3. The samples were heated in the fluid for 24 h at temperatures ranging from 150°C to 325°C. A typical P L-edge spectrum from a film formed at 300°C is shown in Fig. 7C. A polyphosphate is formed on the surface and is similar in character to that formed by the Plint wear rig at 50% relative humidity. There are two differences between the thermal and the antiwear film. First, peak (a) is present in the thermal film but not in the antiwear film. However, for the thermal film, peak (a) is not a broad shoulder like that seen in the low humidity antiwear film (see Fig. 1). It is a resolved feature indicating that the amounts of intermediate phosphates in the thermal film are less than in the tribofilm. Second, the intensity of peak (b) has decreased in intensity relative to peak (c) in the thermal film compared to the 50% relative humidity tribofilm. Based on the work of Yin et al. [29], this decrease in intensity can correlate with a change in the chain length of the polyphosphate formed. Therefore, it appears that the polyphosphate formed in the thermal film is a shorter chain length material compared to the polyphosphate formed in the Plint experiment.

Fig. 8B shows the P K-edge XANES spectrum of the 300°C PH3 thermal sample with three model compounds for spectral comparison. The spectrum is composed of a single peak centered at 2152 eV with a weak shoulder (a) on the low photon energy side, 2148 eV. The strong peak aligns very well with the dominant resonance observed in the model polyphosphates. The weak feature (a) is only apparent on an iron coordinated polyphosphate or P_4O_6 (phosphite) [47]. The origin of the resonance is unclear and does not appear on other organic and transition metal-based polyphosphates. Therefore, K-edge data indicates that the surface film formed thermally is either predominately iron phosphate or phosphite, P_4O_6. The P L-edge data does not clarify the nature of the film. It would appear to be a

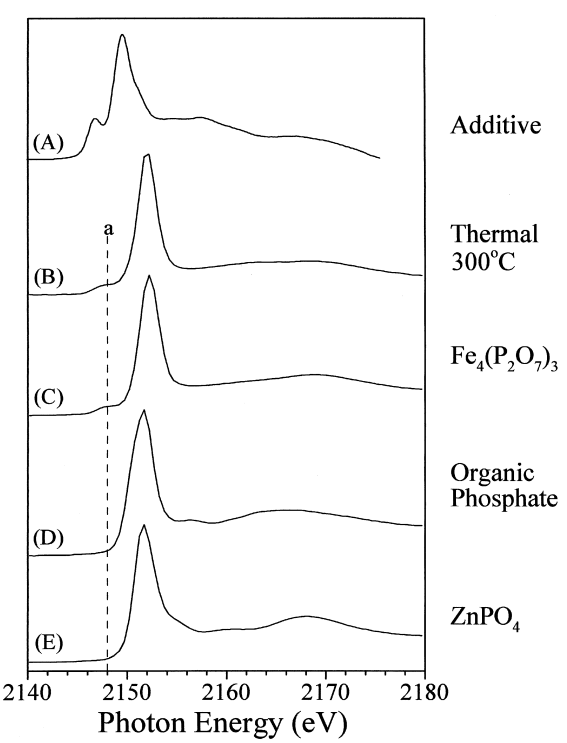

Fig. 8. P K-edge XANES spectra of a thermal film generated by 1% PH3 at 300°C, as compared with model compounds.

polyphosphate but the L-edge data for P_4O_6 has not been reported in the literature. A definitive assignment on the composition of the thermally prepared film is not possible.

The P K-edge spectra for the various films were collected and the corresponding edge jump intensities are plotted in Fig. 9 as a function of digestion temperature. Fig. 9A shows that as the formulated fluid is heated to higher temperatures the amount of polyphosphate formed on the surface increases. Two points can be made about the rate of film growth. First, the film grows exponentially. Second, when the temperature reaches 325°C, there is a rapid drop in the amount of phosphate found on the surface. A visual examination of the coupon showed that the surface film has begun to flake off. As shown in

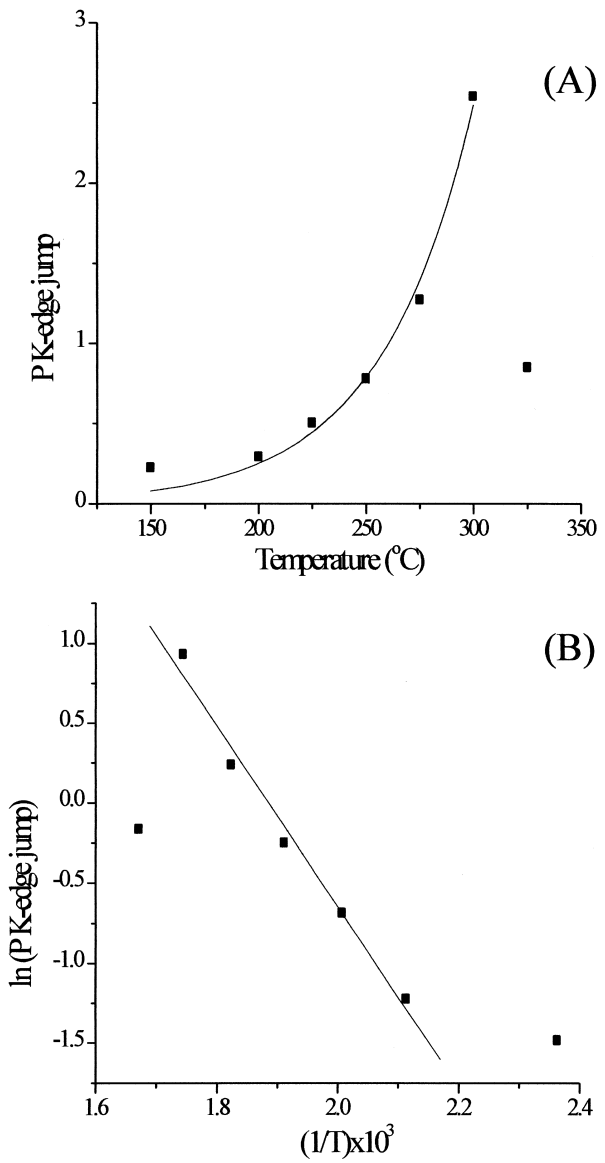

Fig. 9. (A) P K-edge jump as a function of temperature for thermally generated films. (B) Arrhenius plot of the surface concentration of polyphosphate for thermal films. The line of best fit is ln(P K-edge jump) = 10.658 − 5.652(1000/T) (R = 0.9919).

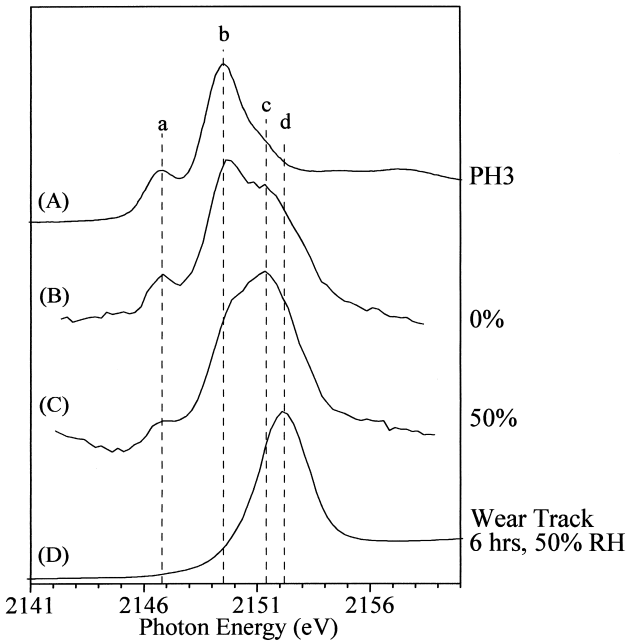

Fig. 10. P K-edge XANES spectra of precipitate from post test oil from two triboexperiments using the Plint wear rig. The test was run at 150°C, 250 N load, 6 h and two different humidities (0% and 50%), as compared to the tribofilm produced by 6 h of rubbing at 50% relative humidity and the starting material.

previous oxidation–corrosion studies of PH3, the additive is effective in protecting the surface from corrosion up to a temperature of 300°C.

Fig. 9B shows the Arrhenius plot obtained from the data in Fig. 9A. Using Eq. (1), an excellent linear relationship is observed between 200°C and 300°C,

$$\ln(\text{P K} - \text{edge jump}) = \ln(A) - E^*/RT \quad (1)$$

giving an activation energy, E^*, of 47 kJ mol^{-1}. The variation below 200°C suggests an alternate growth mechanism is in operation while the variation above 300°C is consistent with severe surface spalling and corrosion.

3.1.7. Precipitate

After two Plint tests, 0% and 50% relative humidity and 6 h of rubbing each, the oil had a cloudy black appearance and appeared to have suspended particulate matter. These oils were filtered and the resulting filter papers were examined using XANES spectroscopy (Fig. 10). Fig. 10B and C show the P K-edge XANES spectra for the two filter papers, along with the additive (Fig. 10A) and a spectrum of the wear track of a Plint sample, Fig. 10D. Spectra of those obtained from the precipitate samples are mixtures of those obtained from the additive and the phosphorus found in the wear track with an additional peak at 2150 eV. Peaks (a) and (b) come from the additive and peak (d) is due to the polyphosphate. Peak (c) is an intermediate phosphate that is generated during the formation of the antiwear film. A closer examination of the

additive (A) shows some evidence of a weak shoulder at a higher photon energy with a position that corresponds to peak c. The spectra of the phosphate found in the wear scar is asymmetric on the low photon energy side of the main resonance, peak d. This asymmetry may reflect the presence of this intermediate in the antiwear film. It is interesting to note that this species is more pronounced at the higher humidity. The chemical shift of this species, peak (c), indicates that the phosphorus is in a lower oxidation state than P(V) possibly an oxidation state of 4 + .

3.1.8. MEPHISTO photoelectron spectromicroscopy

Surfaces were imaged using photoelectron spectromicroscopy [38–40]. Figs. 11 and 12 show the spectromicroscopy images from an oxidation–corrosion coupon and the edge of a wear scar from a Plint reciprocating wear rig. Fig. 11 shows three images from the surface of an oxidation–corrosion sample prepared at 345°C for 24 h with a PH3 formulation. The raw spectromicroscope image, Fig. 11A, shows the general surface morphology of a roughly polished coupon. The polishing marks appear as striations running from the upper right to the lower left. The dark band running across the sample is due to a depression where the oxide has spalled off. Due to the incident angle of the photon beam, 60° to the sample normal, features that are below the plane of the surface are not observed because they are not illuminated by the synchrotron radiation source.

Fig. 11B and C show the difference image for iron distribution map on the surface and the corresponding Fe $M_{2,3}$-edge micro-XANES spectrum taken in the brightly illuminated region in the lower right, respectively. A strong resonance is observed at approximately 58.8 eV (uncalibrated energy scale) which is due to the presence of iron oxide. Outside of the dark band discussed above, the difference image in Fig. 11B shows that the iron oxide is distributed relatively uniformly on the surface.

Fig. 11D and E show the corresponding P $L_{2,3}$-edge difference image and micro-XANES spectrum. The spectra in Fig. 11E are very characteristic of a polyphosphate. Two resonance are observed at approximately 139.1 and 147 eV (uncalibrated energy scale) which qualitatively agree with the spectra of the thermal polyphosphate film shown in Fig. 7. In order to study the distribution of phosphate on the surface, two images were recorded on and off the first resonance whose photon energies are shown by the vertical lines in Fig. 11E. The difference image in Fig. 11D shows that the polyphosphate, as evidenced by the bright patches, is not uniformly distributed on the surface. When compared to the raw image in Fig. 11A, the bands of phosphate seem to correspond to the striations that are caused, possibly, by the polishing. It is unclear from the images if the polyphosphate is forming on the crests of the marks or in the valleys between these surface marks.

Fig. 12A–F show the raw image and corresponding difference images for various molecular species found at

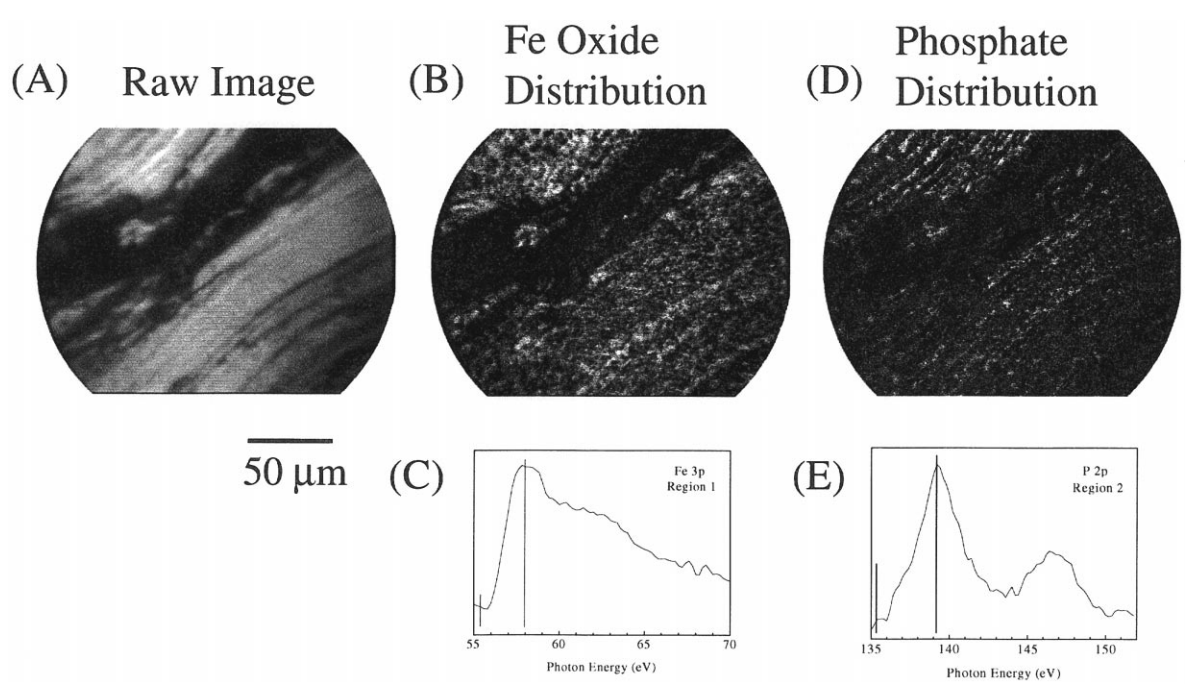

Fig. 11. Photoelectron microimages and spectra of a thermal film prepared using 1% PH3 at 345°C and 24 h. Images B and D are of the iron oxide and phosphate distribution, respectively. These distribution maps were obtained by digitally subtracting an image acquired at 56.5 eV (Fe) and 133.5 eV (P) (pre-edge) from one taken at 58 eV (Fe 3p) and 139.2 (P 2p) (on-edge) (uncalibrated photon energy scale). In these maps, white represents iron oxide or phosphate, black represents their absence.

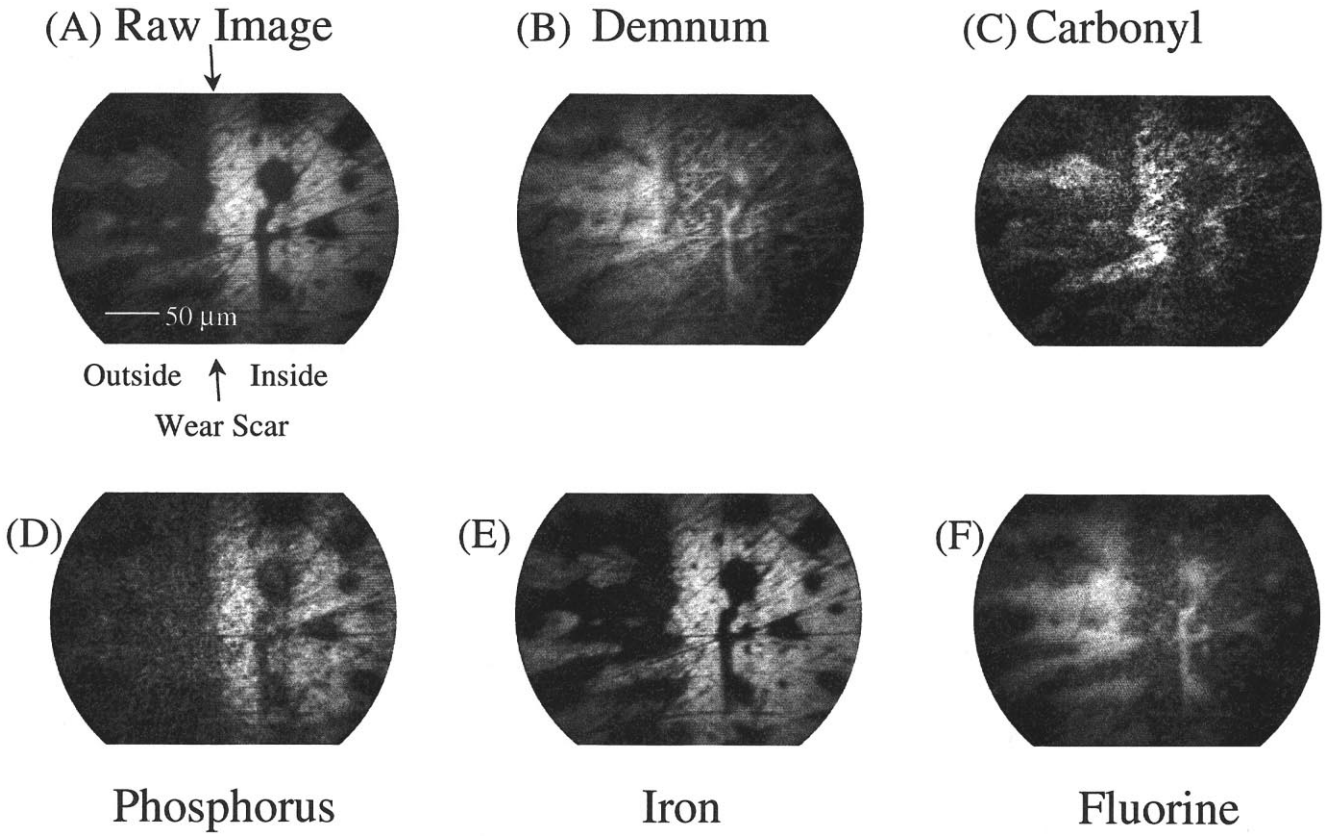

Fig. 12. Photoelectron microimages of a tribofilm prepared using 1% PH3 at 150°C, 250 N load, 2 h and 50% relative humidity. (B) distribution map of Demnum, obtained subtracting an image at 283.7 eV from one at 293.8 eV; (C) distribution map of carbonyl, obtained subtracting an image at 283.7 eV from one at 285.9 eV; (D) distribution map of phosphorus, obtained subtracting an image at 133 eV from one at 140 eV; (E) distribution map of iron, obtained subtracting an image at 703 eV from one at 708 eV; (F) distribution map of fluorine, obtained subtracting an image at 685 eV from one at 692 eV.

the edge of a wear scar from a Plint experiment run with the PH3 additive at 150°C, 2 h, 250 N load, and 50% relative humidity. Fig. 12A shows the raw image at the edge of the wear scar. The edge is apparent by the discontinuous surface film. The dark regions in the left half of the image (outside of the wear scar) are due to the presence of formulated Demnum that was not cleaned off the surface. A closer look within the wear scar shows the presence of scratches on the surface which have no preferred orientation. Fig. 12B shows the difference image for the distribution of Demnum on the surface. Outside of the wear scar, the fluid appears uniformly distributed. Within the wear scar, the Demnum appears to be distributed over the entire scar with higher concentrations along the surface scratches seen in Fig. 12A.

Fig. 12C shows the carbonyl distribution within the wear scar by obtaining the difference image for the carbonyl band, C 1s $\rightarrow \pi^*$. It is apparent that there is an enhancement in the carbonyl distribution at the edge of the wear scar. Similar experiments with unformulated Demnum (unpublished data) have shown the same results. Using XPS and FTIR, various groups [14,41,42] have shown the presence of a carbonyl species on the surface of iron that has interacted with a PFPAE by the formation of acyl fluorides. The enhancement at the edge of the wear scar may be related to turbulence in the fluid caused by the reciprocating motion of the tribometer. The reactive acyl fluorides are swept to the edges of the wear scar at which point they have an opportunity to react with the surface.

Fig. 12D–F show the distribution of phosphate, iron and fluorine, respectively, around the wear scar of the Plint sample. Fig. 12D shows the phosphorus distribution on the surface. Micro-XANES spectra showed that the phosphorus material within the wear scar is a polyphosphate. Fig. 12E and F show the iron and fluorine distribution. Because of the inherently poor photon resolution at $\sim$700 eV photon energy and broad natural linewidths (due to a short lifetime and vibrational broadening) it is not possible to differentiate between different Fe and F molecular species on the surface. It is noteworthy, however, that the iron and fluorine give correlated images that are associated with the edge of the wear scar, i.e., the iron signal is high the fluorine signal is low and vice versa.

3.1.9. Mechanism

The interaction of PH3 with the surface leads to the formation of lubricious films that help protect the surface in a tribological environment. The nature of the lubricious

film is that of a long chain length polyphosphate. In order to form this film, mechanochemical shear, temperature, presence of oxygen and moisture all play essential roles in the creation and stability of the film. Fig. 7 and Table 1 show that oxygen was the first component required to form a good lubricious film. When oxygen was eliminated from the system (fluid and atmosphere), a poor surface film with little protective properties was formed. The second important component was the presence of moisture. As exhibited in Figs. 1 and 2, when moisture was eliminated from the surrounding environment, the surface film formed was thin (on the order of 1–2 nm) relative to the film formed at higher humidity (3–4 nm). Also, in the absence of moisture, the film contained a large amount of unreacted and intermediate material and the film was unstable over long rubbing times. The increased stability at high humidity can be explained by two mechanisms. First, the higher humidity combined with shear induced bond scission allows for the hydrolysis of the additive and formation of a thicker antiwear film. Second, Liang et al. [43,44] showed that at higher humidity PFPAEs form carboxylate multilayers that improve the overall wear performance. The third key component for the formation of a good antiwear films is temperature. Fig. 5 shows that the formation of an antiwear film at low humidity was influenced by the operating temperature. At temperatures less than 150°C and above 200°C, the PH3 formed a very thin film. Whereas, at high humidity, temperature did not have as pronounced an effect on film thickness and lubricity. At low temperatures (125°C) and high humidity (50%), the film was composed of very long chain polyphosphate with a large amount of unreacted material. At temperatures of 150°C and above, the film, as discussed above, was a long chain length polyphosphate with little evidence of unreacted material.

$$PH_3 \underset{H_2O}{\overset{O_2}{\rightarrow}} [P_nO_{3n+1}]^{n+2}$$

In the consideration and development of any phosphorus based PFPAE additives, it is important to realize that several environmental factors play important role in the lubricious properties of the film. First, oxygen is required to form the polyphosphate surface film. Second, moisture is required to hydrolyze the additive and drive the reaction to completion. Third, the phosphorus additive is not very stable and functions over a very limited temperature regime at lower humidity. At high humidity, additive's effectiveness is not strongly dependent on temperature and the observed antiwear properties are due to the nature of the fluorinated fluid.

4. Conclusions

The combination of P K- and L-edge XANES spectroscopy and photoelectron spectromicroscopy have been used to characterize the surface films produced by a Plint reciprocating wear rig. Several general conclusions can be drawn from the presented results.

- The addition of a soluble PFPAE additive enhances the antiwear properties of the base fluid. For the PH3 additive, the P L-edge and K-edge XANES spectra showed that the additive forms a long chain length polyphosphate within a wear scar produced by a Plint wear rig.
- In dry conditions, a wear improvement of ~325% between unformulated and formulated fluid was observed. There is no marked improvement at high humidity. The amount of overall wear is higher at the lower humidity by about 25% when compared to high humidity.
- It was shown that environmental factors, such as oxygen, presence of moisture and temperature, play essential roles in the formation of a good stable lubricious film. First, it was found that oxygen was required to drive the reaction PH3 → polyphosphate. Second, even with oxygen present, hydrolysis due to the presence of moisture when combined with a molecular shear mechanism due to the tribological environment was required to drive the reaction to completion. Third, at low humidity, PH3 had a very narrow useful temperature range of 150°C to 200°C under these accelerated test conditions.
- Photoelectron spectromicroscopy has been applied to show the spatial distribution of the PH3 additive. For a thermally generated film, the phosphate was observed to be concentrated within the polishing marks on the steel substrate. For a tribological film, the polyphosphate was found to reside within the wear scar but not outside.

Acknowledgements

This work was supported by the Materials and Manufacturing Directorate of the Air Force Research Laboratory, Wright Patterson Air Force Base, OH. The authors would like to thank Dr. K.C. Eapen and Mr. G.W. Fultz of the University of Dayton Research Institute for the formulated fluid. The authors are grateful to Dr. J. Zabinski for his thought provoking comments. The photoelectron spectromicroscopy work was partially funded by Fonds National Suisse de la Recherche Scientifique, by the Ecole Polytechnique Fédérale de Lausanne, and by the Consiglio Nazionale delle Ricerche — Instituto di Struttura della Materia. We are grateful to the staff of the Canadian Synchrotron Radiation Facility (CSRF) and the Synchrotron Radiation Center (SRC), University of Wisconsin, Madison for their technical support and the National Science Foundation (NSF) for supporting the SRC under Award #DMR-95-31009.

References

[1] W.H. Gumprecht, ASLE Trans. 9 (1966) 24.
[2] D. Sianesi, V. Zamboni, R. Fontanelli, M. Binaghi, Wear 18 (1971) 85.

[3] C.E. Snyder Jr., R.E. Dolle Jr., ASLE Trans. 19 (1976) 171.
[4] W.R. Jones Jr., C.E. Snyder Jr., ASLE Trans. 23 (1980) 253.
[5] K.J.L. Paciorek, R.H. Kratzer, J. Fluorine Chem. 67 (1994) 169.
[6] R.J. Waltman, G.W. Tyndall, Trib. Lett. (in press).
[7] C.E. Snyder, L.J. Gschwender, C. Tamborski, Lubr. Eng. 37 (1981) 344.
[8] W. Morales, NASA TP 2774 (1987) .
[9] D.J. Carré, ASLE Trans. 29 (1985) 121.
[10] M.J. Zehe, O.D. Faut, Tribol. Trans. 33 (1990) 634.
[11] P.H. Kasai, Macrocolecules 22 (1992) 6791.
[12] P.H. Kasai, P. Wheeler, Appl. Surf. Sci. 52 (1991) 91.
[13] P.H. Kasai, W.T. Tang, P. Wheeler, Appl. Surf. Sci. 51 (1991) 201.
[14] P.J. John, J. Liang, J. Vac. Sci. Technol. A 12 (1994) 199.
[15] B. Çavdar, J. Liang, P.J. John, Tribol. Trans. 39 (1996) 779.
[16] S. Mori, W. Morales, Wear 132 (1989) 111.
[17] S. Mori, W. Morales, Tribol. Trans. 33 (1990) 325.
[18] P. Herrera-Fierro, W.R. Jones Jr., S.V. Pepper, J. Vac. Sci. Technol. A 11 (1993) 354.
[19] J.H. Sanders, J.N. Cutler, G. John, Appl. Surf. Sci. (in press).
[20] J.N. Cutler, J.H. Sanders, G.W. Fultz, K.C. Eapen, Tribol. Lett. (in press).
[21] J.N. Cutler, J.H. Sanders, G. John, Tribol. Lett. 4 (1998) 149.
[22] L.J. Gschwender, C.E. Snyder Jr., G.W. Fultz, Lubr. Eng. 49 (1993) 702.
[23] L.H. Helmick, L.J. Gschwender, S.K. Sharma, C.E. Snyder Jr., J. C Liang, G.W. Fultz, Tribol. Trans 40 (1997) 393.
[24] P.J. John, J. Liang, J.N. Cutler, Tribol. Lett. (in press).
[25] M. Masuko, N. Takeshita, H. Okabe, Tribol. Trans. 38 (1995) 679.
[26] L.J. Gschwender, S.K. Sharma, C.E. Snyder Jr., L. Helmick, G.W. Fultz, B. Schreiber, Tribol. Trans. 41 (1998) 78.
[27] L. Gschwender, C.E. Snyder Jr., M. Oleksiuk, M. Koehler, Tribol. Trans. 39 (1996) 368.
[28] T.N. Wittberg, C.A. Svisco, W.E. Moddeman, Corr. 36 (1980) 517.
[29] Z. Yin, M. Kasrai, M. Fuller, G.M. Bancroft, K. Fyfe, K.H. Tan, Wear 202 (1997) 172, and references therein.
[30] Z. Yin, M. Kasrai, G.M. Bancroft, K. Fyfe, M.L. Colaianni, K.H. Tan, Wear 202 (1997) 192.
[31] M. Fuller, Z. Yin, M. Kasrai, G.M. Bancroft, E.S. Yamaguchi, P.R. Ryason, P.A. Willermet, K.H. Tan, Tribol. Int. 30 (1997) 305.
[32] M. Kasrai, J.N. Cutler, K. Gore, G. Canning, G.M. Bancroft, K.H. Tan, Tribol. Trans. 41 (1998) 69.
[33] J.N. Cutler, J.H. Sanders, P.J. John, N. Forester (unpublished results).
[34] J. Stöhr, NEXAFS Spectroscopy, Springer Series in Surface Science, Vol. 25, Springer-Verlag, Berlin, 1992.
[35] C. Tamborski, C.E. Snyder, Jr., J.B. Christian, United States Patent 4,454,349, 1984.
[36] G.M. Bancroft, Can. Chem. News 44 (1992) 15.
[37] M. Kasrai, Z. Yin, G.M. Bancroft, K.H. Tan, J. Vac. Sci. Technol. A 11 (1993) 2694.
[38] G. De Stasio, M. Capozi, G.F. Lorusso, P.A. Baudat, T.C. Droubay, P. Perfetti, G. Margaritondo, B.P. Tonner, Rev. Sci. Instrum. 69 (1998) 2062.
[39] G. De Stasio, L. Perfetti, B. Gilbert, O. Fauchoux, M. Capozi, P. Perfetti, G. Margaritondo, B.P. Tonner, Rev. Sci. Instrum. 70 (1999) 1740.
[40] G. De Stasio, B. Gilbert, L. Perfetti, T. Nelson, M. Capozi, P.A. Baudat, F. Cerrina, B.P. Tonner, G. Margaritondo, Rev. Sci. Instrum. 69 (1998) 3106.
[41] T.E. Karis, V.I. Novotny, R.D. Johnson, J. Appl. Polym. Sci. 50 (1993) 1357.
[42] J. Liang, H. Spikes (unpublished data).
[43] J. Liang, B. Cavdar, S.K. Sharma, Tribol. Lett. 3 (1997) 107.
[44] J. Liang, Y.S. Tung, D.O. Henderson, L.S. Helmick, Tribol. Lett. 3 (1997) 113.
[45] Z. Yin, PhD Thesis, The University of Western Ontario, London, Canada, 1995.
[46] T.W. Del Pesco, Perfluoroalkylethers, in: R.L. Shubkin (Ed.), Synthesis Lubircants and High Performance Fluids, Vol. 155, Marcel Dekker, New York, 1993.
[47] G. Küper, R. Chauvistré, J. Hormes, F. Frick, M. Jansen, B. Lüer, E. Hartmann, Chem. Phys. 165 (1992) 405.